Available online at www.sciencedirect.com
ScienceDirect
Applied Catalysis B: Environmental 81 (2008) 49–55
APPLIED CATALYSIS B: ENVIRONMENTAL
www.elsevier.com/locate/apcatb

Study of the synergic effect of sulphate pre-treatment and platinisation on the highly improved photocatalytic activity of TiO_2

M.C. Hidalgo *, M. Maicu, J.A. Navío, G. Colón

Instituto de Ciencia de Materiales de Sevilla (ICMSE), Consejo Superior de Investigaciones Científicas CSIC, Universidad de Sevilla, Américo Vespucio 49, 41092 Sevilla, Spain

Received 26 September 2007; received in revised form 20 November 2007; accepted 24 November 2007
Available online 8 December 2007

Abstract

An important improvement of the photocatalytic activity of sol–gel prepared TiO_2 has been achieved by sulphate pre-treatment, calcination at high temperature and further platinisation of the samples.

The presence of sulphuric acid clearly stabilised TiO_2 surface area against sintering, maintaining at the same time anatase phase until higher calcination temperatures than in non-sulphated samples. Platinisation of the samples with different nominal amounts of platinum (from 0.5 to 2.5 wt%) was performed and the influence of sulphate treatment on the dispersion and deposit size of platinum on the TiO_2 surface was studied.

Characterisation results and photocatalytic activity of these catalysts were compared with those of unmodified TiO_2. Simultaneously sulphated and platinised TiO_2 samples were highly active for phenol degradation, used as model reaction for the photocatalytic studies, having higher activities than only platinised or only sulphated samples. The activity of these samples were several orders of magnitude higher than that of the commercial TiO_2 Degussa P25 (platinised or unmodified) as well, with independence of the nominal amount of platinum of the samples.

A wide characterisation of the samples was performed and correlations between characterisation results and activity properties are reported.

Keywords: Pt/TiO_2; Platinisation; Sulphated TiO_2; Photocatalysis; Phenol oxidation; Metal dispersion

1. Introduction

TiO_2 photocatalysis has been the subject of great interest in the last years as an effective and environmentally friendly method for water and air purification [1–4]. In order to improve the photocatalytic activity of TiO_2 systems different options have been investigated and widely reported in the literature, such as dye-sensitisation [5], control of structure and particle size of the titania [6,7], doping with different anions [8–10] and cations [11,12] or surface modification with noble metals or other semiconductors [13–16]. Among noble metals, platinum has been one of the most used metals for TiO_2 surface modification [13]. The effect of platinisation on the photocatalytic activity of TiO_2 has been a controversial subject in the literature and reported experimental results have been contradictory [13,17,18]. The role of platinum in photocatalysis is still not totally understood and the degree of enhancement of the activity of TiO_2 by platinisation seems to depend highly on the substrate to be degraded [17,19], the properties and amount of deposited Pt [13,20] and structural and morphological properties of original TiO_2 [21,22]. In general it is accepted that in platinised TiO_2 a better separation of charge carriers (electrons and holes) is observed. Moreover, it is assumed that some of the photogenerated electrons would interact with platinum states and be spatially separated from holes [23].

On the other hand, sulphuric acid pre-treament of TiO_2 has been reported to stabilise TiO_2 surface area against sintering and anatase crystalline phase until calcination temperatures as high as 700 °C. In addition, sulphated TiO_2 also presented higher photoactivities than non-sulphated TiO_2 for phenol oxidation [10,24,25]. These results were explained by the creation of bulk oxygen vacancies through a dehydroxylation process of the excess of adsorbed protons during calcination, generating a highly defective material and improving the separation of photogenerated charges and their diffusion to the surface in the photocatalytic process [10].

* Corresponding author. Tel.: +34 954489576; fax: +34 954460665.
E-mail address: mchidalgo@icmse.csic.es (M.C. Hidalgo).

0926-3373/$ – see front matter
doi:10.1016/j.apcatb.2007.11.036

In the present work, sol–gel prepared TiO_2 was modified by sulphate pre-treatment and further platinised with the purpose of obtaining improved photocatalysts combining the effects of both treatments simultaneously. The dispersion and cluster size of platinum on the TiO_2 was affected by sulphate pre-treatment of the surface. A synergic effect was found between sulphation and platinisation leading to an improvement of the photocatalytic activity for phenol photooxidation reaction.

2. Experimental

2.1. Catalyst preparation

TiO_2 was prepared by the hydrolysis of titanium tetraisopropoxide (Aldrich, 97%) in isopropanol solution (1.6 M) by the addition of distilled water (volume ratio: isopropanol/water 1:1). Subsequently the as-generated precipitate was filtered, washed twice with distilled water and dried at 110 °C overnight.

For non-sulphated TiO_2 (Tip NS), the dried precipitate was just calcined at 500 °C for 2 h. For sulphated TiO_2 (Tip S), the dried precipitate was impregnated by a sulphuric acid 1 M solution for 1 h, then filtered again, dried at 110 °C overnight and calcined at 700 °C for 2 h, following the same procedure of our previous work [24]. These calcination temperatures were chosen in order to compare best samples in both series regarding photocatalytic activity for phenol degradation, i.e., 500 °C for non-sulphated TiO_2 and 700 °C for sulphated TiO_2. Calcination at lower temperatures would lead to poor photocatalytic behaviour for both series, especially for the sulphated samples [24].

Platinisation was performed over the calcined TiO_2 samples by photodeposition of platinum from hexachloroplatinic(IV) acid (H_2PtCl_6, Merck 40% Pt) following a modification of a method described elsewhere [15]. Suspensions of the different TiO_2 in distilled water were prepared (5 g TiO_2 L^{-1}) adding isopropanol to act as sacrificial agent (0.3 M final concentration) and the appropriate amount of H_2PtCl_6 for different nominal amounts of deposited Pt (0.5–2.5% weight total to TiO_2) under continuous nitrogen sparging. Photodepositions were performed by illumination of the suspensions for 6 h with a medium pressure mercury lamp (400 W) of photon flux ca. 2.6×10^{-7} Einstein s^{-1} L^{-1} in the region of wavelengths <400 nm. After recovering of the powders by filtration, samples were dried at 110 °C overnight.

To assure reproducibility of the preparation method, selected samples were independently prepared twice, and the reproducibility in structural and morphological as well as in activity results was confirmed.

Hereafter samples will be named by Tip NS or Tip S followed by the amount of platinum on the sample, e.g., Tip S 1.5Pt means sulphated TiO_2 platinised with 1.5 wt% nominal content of platinum.

2.2. Characterisation of the catalysts

The study of the samples by transmission electron microscopy (TEM) provided information about Pt deposits size and dispersion. TEM observations were performed using a Philips CM 200 instrument. The microscope was equipped with a top-entry holder and ion pumping system, operating at 200 kV and given a nominal structural resolution of 0.21 nm. The samples were dispersed in ethanol using an ultrasonicator and dropped on a carbon grid.

Surface characterisation was performed by X-ray photoelectron spectroscopy (XPS). The XPS study was carried out on a Leybold–Heraeus spectrometer (LHS-10), working with a constant pass energy of 50 eV. The spectrometer main chamber, working at a pressure $<2 \times 10^{-9}$ Torr, was equipped with an EA-200 MCD hemispherical electron analyzer with a dual X-ray source working with Al Kα ($h\upsilon$ = 1486.6 eV) at 120 W and 30 mA. C 1s signal (284.6 eV) was used as internal energy reference in all the experiments. Samples were outgassed in the prechamber of the instrument at 150 °C up to a pressure $<2 \times 10^{-8}$ Torr to remove chemisorbed water from their surfaces.

Total platinum content of the samples was determined by X-ray fluorescence spectrometry (XRF) in a Panalytical Axios sequential spectrophotometer with a rhodium tube as the source of radiation. XRF measurements were performed onto pressed pellets (sample included in 10 wt% of wax).

Light absorption properties of the samples were studied by UV–vis spectroscopy. UV–vis spectra were measured on a Varian spectrometer model Cary 100 equipped with an integrating sphere and using $BaSO_4$ as reference. All the spectra were recorded in diffuse reflectance mode and transformed to a magnitude proportional to the extinction coefficient through the Kubelka–Munk function, $F(R_\infty)$. Band-gaps were calculated by using the Kubelka–Munk functions according to the method proposed by Tandom and Gupta [26].

Crystalline phase composition and degree of crystallinity of the samples were estimated by X-ray diffaction (XRD). XRD patterns were obtained on a Siemens D-501 diffractometer with Ni filter and graphite monochromator using Cu Kα radiation (λ = 1.5418 Å). Crystallite sizes of the different phases were estimated from the line broadening of the corresponding X-ray diffraction peaks by using the Scherrer equation. Peaks were fitted by using a Voigt function.

BET surface area and porosity measurements were carried out by N_2 adsorption at 77 K using a Micromeritics ASAP 2010 instrument.

2.3. Photocatalytic runs

The photocatalytic activity of the samples was tested for phenol oxidation, chosen as model reaction. Suspensions of the samples (1 g L^{-1}) in phenol solution (50 ppm) were placed in a batch reactor (200 mL) and illuminated through a UV-transparent Plexiglas® top window (threshold absorption at 250 nm) by an Osram Ultra-Vitalux lamp (300 W) with sun-like radiation spectrum and a main line in the UVA range at 365 nm. The intensity of the incident UVA light on the solution was measured with a PMA 2200 UVA photometer (Solar Light Co.) being ca. 95 W m^{-2}. Magnetic stirring and oxygen flow were used to produce a homogeneous suspension of the catalyst

in the solution. Prior illumination, catalyst–substrate equilibration was allowed by stirring the suspension 20 min in the dark. The evolution of the phenol concentration was measured by UV–vis spectrometry following its 270 nm characteristic band. The activity of the different samples was estimated by using initial degradation rates (30 min) as degradation profiles followed zero-order kinetics during this stage.

Blank experiments were performed in the dark as well as with illumination and no catalyst, without observable change in the initial concentration of phenol in both cases.

3. Results and discussion

3.1. Characterisation of platinised and non-platinised samples

Crystalline phase compositions of all samples were studied by XRD (patterns not shown). Both sample series, the non-sulphated series as well as the sulphated one, showed only anatase phase. In previous studies, it has been shown that sulphuric acid pre-treatment of TiO_2 stabilises anatase phase against sintering and phase transformation into rutile up to calcination temperature as high as 700 °C [10,24]. This stabilisation of anatase phase as well as of surface area could be explained by taking into account the presence of sulphate groups anchored on the TiO_2 precursor before calcination. At this temperature last remaining sulphate groups are removed and afterward calcinations at temperatures higher than 700 °C lead to a fast rutilisation of the TiO_2 samples [24]. In addition, the creation of bulk oxygen vacancies through a dehydroxylation process of the excess of adsorbed protons (Brönsted acid sites) during calcination leads to the generation of a highly defective material [10].

For both series, phase composition was unaltered by platinisation. Anatase crystalline domains for the samples, estimated by the Scherrer equation, are presented in Table 1. Due to the different calcination temperature for sulphated and non-sulphated samples, crystallite size values for both series are different: around 18 nm for non-sulphated TiO_2 and 32 nm for the sulphated one. Platinisation did not significantly change those values as it can be seen in Table 1. Neither the position nor the width of the peaks suffered any appreciable change with platinisation, suggesting that there was not distortion of the original TiO_2 structure due to the doping.

None of the XRD patterns of the platinised samples displayed Pt peaks, since metal sites are expected to be below the detection limit of X-ray analysis even for samples with the highest content in platinum (2.5 wt%).

BET surface area values for the samples are shown in Table 1. Non-sulphated samples presented BET surface area values around 39 $m^2\,g^{-1}$ while sulphated samples presented values around 20 $m^2\,g^{-1}$. These results are in very good agreement with the difference in the anatase crystallite size observed between both series (Table 1). The smaller surface area of the sulphate series can be ascribed to the higher calcination temperature used in the preparation of these samples. However, BET surface area values were not affected by the platinisation process.

Light absorption properties of the samples were studied by UV–vis spectroscopy (spectra not shown for the sake of brevity). Sulphated and non-sulphated series presented similar band-gap values, around 3.2–3.3 eV in any case. Comparison between the diffuse reflectance spectra of platinised and non-platinised samples showed no differences in the UV range. Due to their dark grey colour, platinised samples showed a stronger absorption respect to unmodified samples throughout the visible range.

A summary of XPS results of the different samples is shown in Table 2. Binding energies for Ti $2p_{3/2}$ peaks at 458.6 ± 0.2 eV can be assigned to Ti^{4+} in TiO_2 lattice. However, in many samples the ratio O/Ti is bellows stoichiometric value (O/Ti = 2), and thus a certain number of oxygen vacancies is expected for these samples. The amount of oxygen vacancies seems to be higher in the non-sulphated series where lower O/Ti ratios are found. On the contrary,

Table 1
Summary of characterisation results

Sample	S_{BET} (m^2/g)	Anatase crystallite size (nm)[a]	Main Pt particle size range (nm)[b]
Tip NS	40.6	17	–
Tip NS 0.5Pt	38.2	18	n.d.
Tip NS 1Pt	37.8	17	3–5
Tip NS 1.5Pt	39.1	19	3–6
Tip NS 2Pt	37.1	24	3–5
Tip NS 2.5Pt	43.0	18	2–4
Tip S	19.1	31	–
Tip S 0.5Pt	19.5	32	n.d.
Tip S 1Pt	18.1	30	1–3
Tip S 1.5Pt	19.1	31	2–4
Tip S 2Pt	19.3	28	2–3
Tip S 2.5Pt	20.6	29	3–5

n.d.: not determined.
[a] Estimated by using the Scherrer equation.
[b] Range of platinum deposit sizes estimated by TEM observations using the same extension of surface area for each sample.

Table 2
Summary of XPS results for the different samples

Sample	Binding energy (eV)		Pt (at.%)	C (at.%)	O/Ti
	Ti $2p_{3/2}$	O 1s			
Tip NS	458.6	530.1	–	4.53	1.89
Tip NS 0.5Pt	458.7	530.0	0.07	7.58	1.92
Tip NS 1Pt	458.5	530.0	0.20	9.36	1.95
Tip NS 1.5Pt	458.6	530.1	0.30	7.89	1.92
Tip NS 2Pt	458.4	529.8	0.38	8.79	1.93
Tip NS 2.5Pt	458.4	529.6	0.39	7.42	1.96
Tip S	458.5	530.4	–	4.60	1.70
Tip S 0.5Pt	458.6	529.7	0.21	8.22	2.06
Tip S 1Pt	458.5	530.2	0.62	6.48	1.94
Tip S 1.5Pt	458.5	529.7	0.78	5.16	1.95
Tip S 2Pt	458.9	530.6	0.37	7.74	2.00
Tip S 2.5Pt	458.9	529.6	0.59	5.66	1.99

Table 3
Platinum content on the different samples: weight total content (XRF) and weight surface content (XPS)

Sample	Nominal	Pt (wt%)	
		XRF	XPS
Tip NS 0.5Pt	0.5	0.48	1.15
Tip S 0.5Pt	0.5	0.37	1.73
Tip NS 1Pt	1	1.04	1.44
Tip S 1Pt	1	0.77	4.80
Tip NS 1.5Pt	1.5	1.40	2.36
Tip S 1.5Pt	1.5	1.49	6.00
Tip NS 2Pt	2	1.86	2.98
Tip S 2Pt	2	1.85	2.71
Tip NS 2.5Pt	2.5	2.82	3.05
Tip S 2.5Pt	2.5	2.63	4.65

sulphated series present ratios closer to the stoichiometric value after platinisation. The loss of the reported oxygen vacancies would take place during the platinisation process, when these vacancies would be annihilated on the photodeposition step while platinum is reduced.

Regarding the XPS oxygen region, for all samples O 1s peak is found at binding energies of 529.9 ± 0.3 eV together with a small shoulder at higher binding energies (ca. 532 eV). This main peak can be assigned to lattice oxygen while the shoulder could be associated to oxygen as carbonate species as well as surface hydroxyl groups which seem to be present in all samples [27].

For all samples, XPS analysis of the S 2p region was also performed and no peak was detected; indicating that the amount of S on the surface of the samples was below the detection limit of the instrument and can be considered negligible for both series. These results show that for sulphated samples most of sulphate groups were removed during their calcination at 700 °C, in agreement with results in Ref. [24].

Total platinum content in the samples was determined by XRF (values shown in Table 3). Bulk content of platinum was in most cases just slightly lower than the theoretical nominal content chosen in the preparation of the samples (0.5–2.5 wt%), evidencing that right platinisation conditions were employed during the photodeposition.

For samples with the same nominal platinum content, XPS results showed a higher superficial content of the metal for sulphated samples, as it can be seen in Table 3, with the exception of sample Tip S 2Pt. Even taking into account the different BET surface area between both series (Table 1) sulphated samples showed a higher surface amount of platinum than non-sulphated ones. XPS is a surface sensitive technique and can give information about how well the particles of platinum are dispersed over the TiO_2. For two samples with the same total amount of platinum, the sample with a higher dispersion of the metal on the surface will show a higher signal peak for platinum in the XPS spectrum because the corresponding TiO_2 surface will be more largely covered [28]. Therefore, it can be assumed that sulphate pre-treatment of TiO_2 made the dispersion of platinum on the TiO_2 surface higher (this conclusion is also supported by the TEM results as it will be shown later) even considering the differences in surface area of the samples. This tendency is presented in Fig. 1, where XFR versus XPS platinum content has been represented.

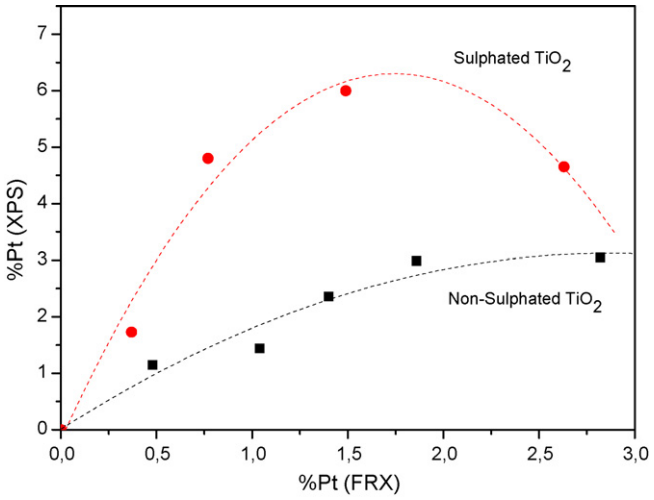

Fig. 1. Bulk platinum content (measured by FRX) vs. surface platinum content (measured by XPS) for the two series of samples (sulphated and non-sulphated).

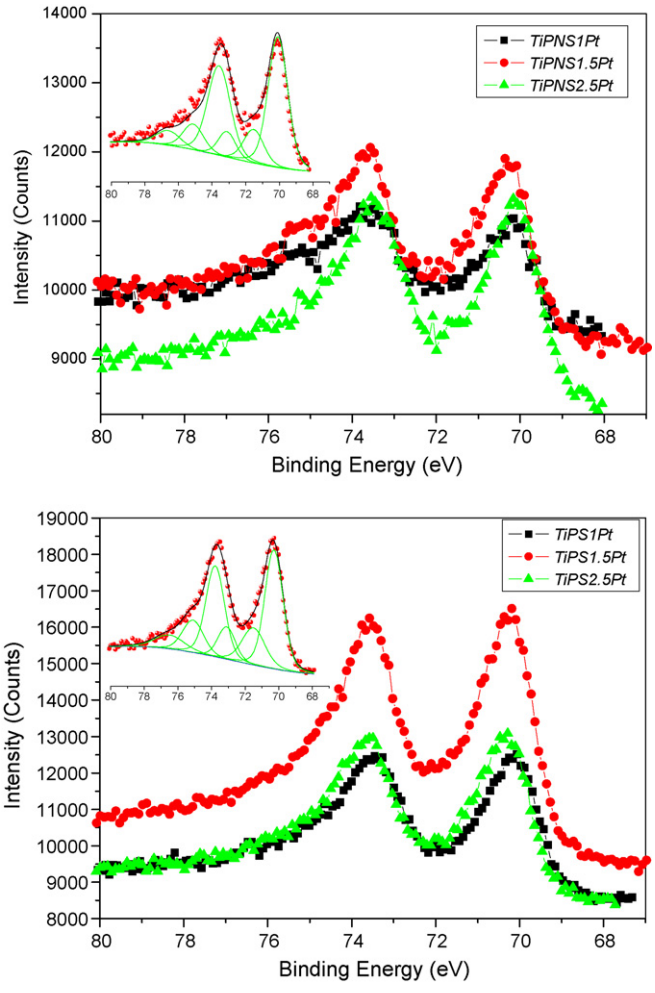

Fig. 2. XPS spectra in the Pt 4f region for the indicated samples.

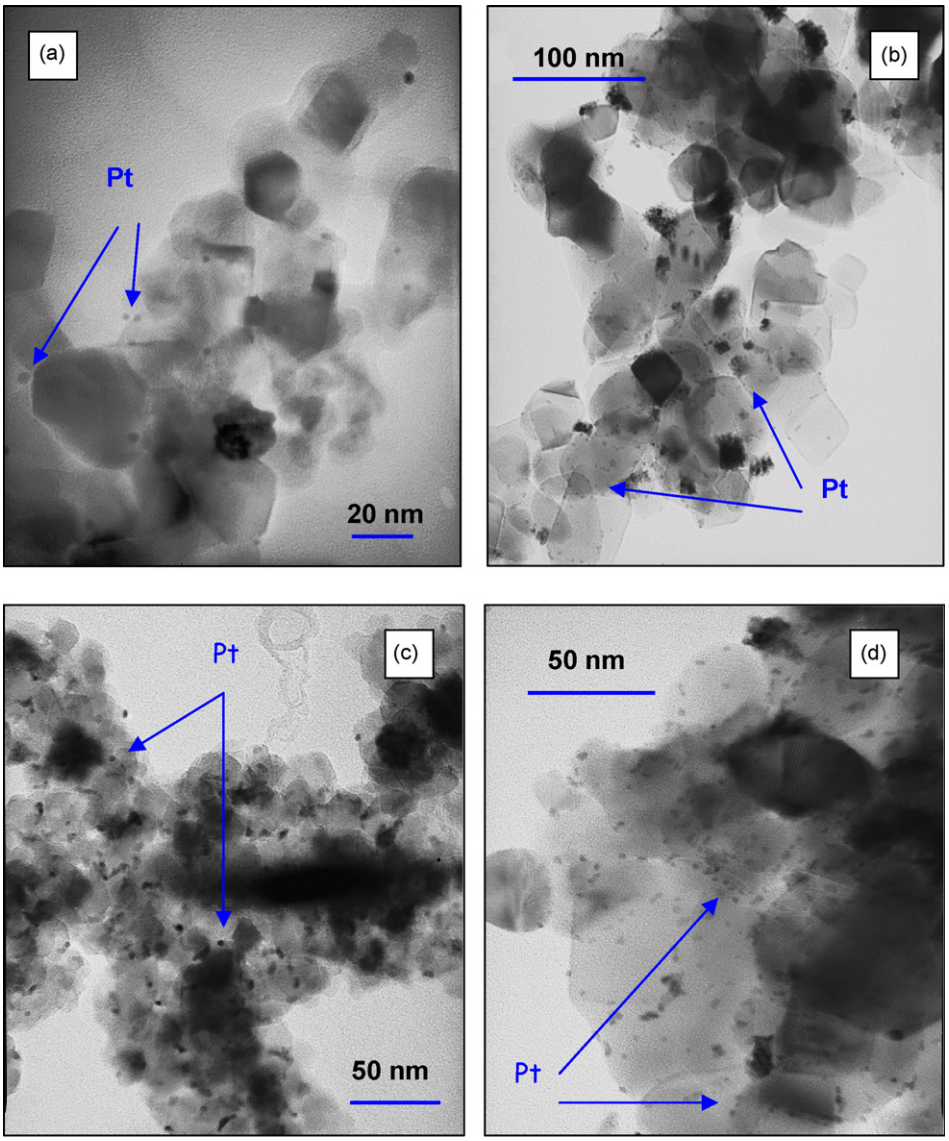

Fig. 3. TEM micrographs of selected samples: Tip NS 1Pt (a), Tip S 1Pt (b), Tip NS 1.5Pt (c) and Tip S 1.5Pt (d).

The slope at low metal content (up to 1.5 wt% Pt) for the sulphated series is around three times larger than the slope for the non-sulphated series. At platinum content higher than 2%, a certain agglomeration is observed for sulphated series, leading to a significantly decrease in the XPS value with respect to XRF (Fig. 1). This agglomeration is observed for non-sulphated series at the earliest platinum content, showing an almost linear correspondence between both values.

The determination of the nature and oxidation state of Pt species (Pt^0, Pt^{2+} and Pt^{4+}) is also normally accomplished by using XPS technique and in particular by means of the Pt 4f peak study. Information concerning the metal oxidation state in platinum doping is very important since this has been reported as one of the factors with a stronger influence in the photocatalytic properties of Pt-doped TiO_2 systems, being Pt^0 generally accepted as the state of platinum leading to most favourable results in photocatalytic activity [20,28]. Fig. 2 shows Pt 4f region for three selected pairs of samples (sulphated and non-sulphated). The Pt 4f signal consisted in three pairs of doublets (inset in Fig. 2). The most intense doublet (ca. 70.2 and 73.6 eV) would correspond to metallic Pt. Other two less prominent doublets can be resolved with $4f_{7/2}$ signals located at ca. 71.5 and 73.1 eV. These other contributions would be associated to Pt^{2+} and Pt^{4+}, respectively [29,30]. From these results we can conclude that for both series platinum on the samples is mainly in the form of Pt^0 with a small amount of Pt^{2+} and Pt^{4+}.

The study of the platinised samples by TEM also can give an indication of Pt deposits size and dispersion. Micrographs of selected samples are presented in Fig. 3. All photodeposited platinum-islands were spherical, however as it can be observed metal deposits on sulphated samples have a higher dispersion on the TiO_2 particles, in agreement with XPS results. An estimation of the main average platinum particle size of the samples was made by counting platinum particles in a high number of TEM micrographs and the values are shown in Table 1. It can be inferred that samples with sulphated pre-treatment presented smaller platinum deposits. Platinum

particle size also increased slightly when increasing the platinum content in the samples.

The relatively high dispersion of Pt obtained for the sulphated TiO_2 can be related with the features of the oxide surface and the interaction between platinum precursor and the titania surface [31]. Tentatively, it can be suggested that sulphation could change either adsorption properties of the TiO_2 regarding hexachloroplatinic(IV) acid the platinum precursor, or the zero point of charge (ZPC) of the surface leading to a less degree of agglomeration of the titania particles and therefore increasing the surface area available for adsorption and deposition of the metal ions. In addition, and perhaps more importantly, the particular structural and electronic features of the sulphated samples [10], would directly affect to the photoreduction process.

3.2. Photocatalytic activity for phenol degradation

The photocatalytic activity of the samples was tested in the reaction of photooxidation of phenol. Initial decomposition rates for this reaction over the different samples versus bulk platinum content is shown in Fig. 4 (upper figure). All platinised samples showed significantly higher photocatalytic activity than non-modified TiO_2 for this model reaction. It can be seen that the photocatalytic activity of the samples increased with the platinum content reaching a maximum around 1–1.5% of Pt for both series (sulphated and non-sulphated samples) and decreased for higher Pt content. This subsequent decreasing evolution would be related with the agglomeration process that takes place at high Pt loading shown in Fig. 1. As it can be seen in Fig. 4, the enhancement by platinisation was higher in the case of TiO_2 with sulphate pre-treatment for every platinum content, showing a synergic effect between sulphate pre-treatment and platinisation in the improvement of the photocatalytic activity of sol–gel prepared TiO_2 for the reaction of photooxidation of phenol. The improvement is even more remarkable if we consider the activity per surface area unit of catalyst (lower figure in Fig. 4) taking into account the different BET surface area of the samples in both series.

Sulphate pre-treatment of TiO_2 surface improved the efficiency of further platinisation, producing a better dispersion and lower particle size of the metal as it has been seen in the previous section. This shows that when comparing different Pt-doped TiO_2 samples, not only is important the amount of metal but also the dispersion and size of the deposits, and this can be the origin of differences in the activities of samples with the same amount of platinum found in the literature [13]. These results show that metal dispersion and deposits size in Pt–TiO_2 systems can be different even using identical photodeposition conditions and will depend in great extent on the surface properties of the original TiO_2.

It is nowadays accepted that noble metal nanoparticles as platinum deposited on the TiO_2 surface are effective traps for photogenerated electrons due to the formation of a Schottky barrier at the metal–semiconductor contact. These electrons can improve the rate of reduction of oxygen (cathodic half-reaction in the photocatalytic process) and reduce the probability of

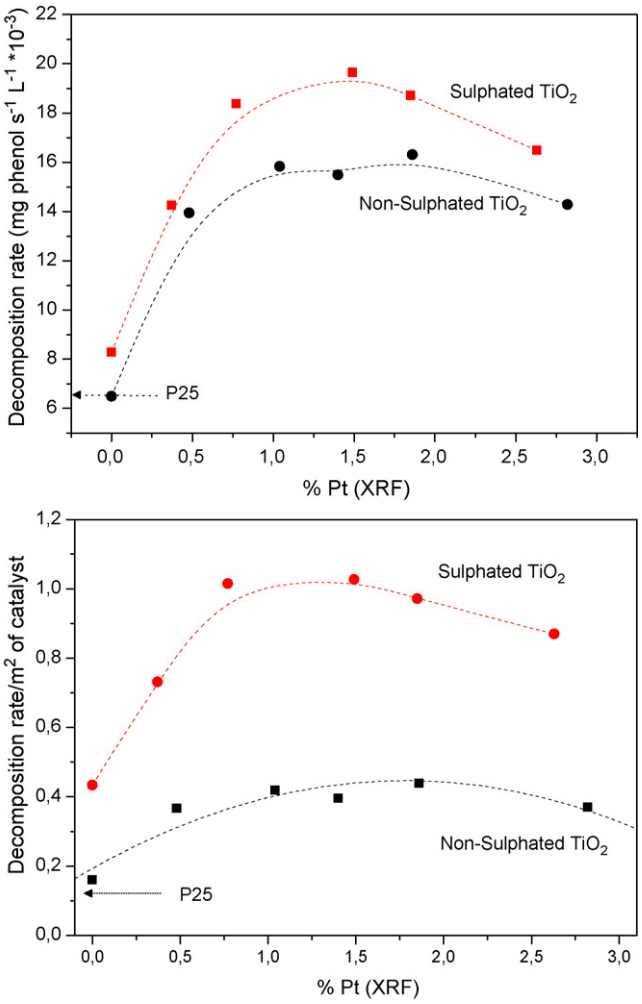

Fig. 4. Initial reaction rate for phenol photooxidation over the catalysts with different platinum content (upper figure) and initial reaction rate for phenol photooxidation per surface area unit of catalyst (lower figure). $[Phenol]_0 = 50$ mg L^{-1}, $V = 0.2$ L, [catalyst] = 1 g L^{-1}, $I = 95$ W m^{-2}.

electron–hole recombination [13,15]. In agreement with the results obtained, the efficiency of platinum deposits as electron traps will be improved by a higher dispersion and lower particle size of the metal.

It is worth to be noticed that all samples are significantly more active than commercial TiO_2 Degussa P25 or platinised TiO_2 Degussa P25 (Fig. 4). Moreover, some of us reported no improvement of the activity for phenol degradation for this commercial TiO_2 by platinisation [22].

Fig. 5 shows activity of the samples versus surface content of platinum (calculated by XPS results). It can be observed that the samples with the highest platinum content on the surface presented the highest activity for phenol degradation, what suggest that the factor influencing the activity is the amount of platinum seen on the surface with independence of the bulk or total amount of the metal. Thus, although certain agglomeration is observed for sulphated series after 2% platinum loading, the higher metal dispersion in this series still induces a progressively increase in the photoactivity. At the same time, this surface amount of platinum will also depend on the surface

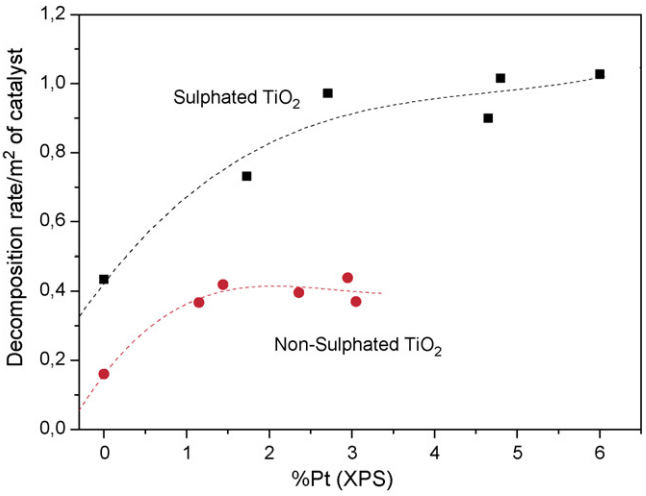

Fig. 5. Initial reaction rate for phenol photooxidation for the catalysts with different surface platinum content measured by XPS $[Phenol]_0 = 50$ mg L^{-1}, $V = 0.2$ L, [catalyst] = 1 g L^{-1}, $I = 95$ W m^{-2}.

properties of TiO_2 and, as it has been shown in this work, can be improved by sulphate pre-treatment.

4. Conclusions

A synergic affect between platinisation and sulphate pre-treatment of TiO_2 was found for the photocatalytic activity of sol–gel prepared TiO_2. Samples simultaneously sulphated and platinised obtained a remarkable improvement of the photocatalytic activity for phenol degradation.

Sulphated pre-treatment clearly stabilised TiO_2 surface area against sintering, maintaining at the same time anatase phase until a high calcination temperature (700 °C). Sulphation of TiO_2 influenced results of platinisation, producing a higher dispersion and smaller average deposit size of platinum. Both factors contributed to the higher photocatalytic activity of these samples compared to the non-sulphated series. Optimum content of platinum was found between 1 and 1.5 wt%.

For both series (sulphated and non-sulphated), best photocatalytic activities were obtained for samples with the highest surface metal content, showing that the activity is influenced by surface amount more than by bulk amount of platinum.

The activity of these samples were several orders of magnitude higher than that of the commercial TiO_2 Degussa P25 (platinised or unmodified) as well, with independence of the nominal amount of platinum of the samples.

Acknowledgements

This research was financed by the Spanish Ministerio de Educación y Ciencia (project ref. CTQ2004-05734-C02-02). Partial financial support by the Junta de Andalucía (P.A.I. group reference FQM181) is also acknowledged. M.C.H. thanks the Spanish Ministerio de Educación y Ciencia (Ramón y Cajal Programme N.2003/116) for financial support.

References

[1] A. Fujishima, T.N. Rao, D.A. Tryk, J. Photochem. Photobiol. C 1 (2000) 1.
[2] O. Carp, C.L. Huisman, A. Reller, Prog. Solid State Chem. 32 (2004) 33.
[3] V. Augugliaro, M. Litter, L. Palmisano, J. Soria, J. Photochem. Photobiol. C 7 (2006) 127.
[4] M. Kitano, M. Matsuoka, M. Ueshima, M. Anpo, Appl. Catal. A 325 (2007) 1.
[5] K. Kalyanasundaram, M. Gratzel, Coord. Chem. Rev. 77 (1998) 347.
[6] M. Tomkiewicz, Catal. Today 58 (2000) 115.
[7] M.C. Hidalgo, M. Aguilar, M. Maicu, J.A. Navío, G. Colón, Catal. Today 129 (2007) 50.
[8] S. Sakthivel, H. Kisch, Angew. Chem. Int. Ed. 42 (2003) 4908.
[9] R. Asahi, T. Morikawa, T. Ohwaki, K. Auki, Y. Taga, Science 293 (2001) 269.
[10] G. Colón, M.C. Hidalgo, G. Munuera, I. Ferino, M.G. Cutrufello, J.A. Navío, Appl. Catal. B 63 (2006) 45.
[11] C. Adán, A. Bahamonde, M. Fernández-García, A. Martínez-Arias, Appl. Catal. B 72 (2007) 11.
[12] G. Colón, M. Maicu, M.C. Hidalgo, J.A. Navío, Appl. Catal. B 67 (2006) 41.
[13] S.K. Lee, A. Mills, Platinum Met. Rev. 47 (2003) 61.
[14] V. Iliev, D. Tomova, L. Bilyarska, G. Tyuliev, J. Mol. Catal. A 263 (2007) 32.
[15] D. Hufschmidt, D. Bahnemann, J.J. Testa, C.A. Emilio, M.I. Litter, J. Photochem. Photobiol. A 148 (2002) 223.
[16] I. Robel, V. Subramanian, M. Kuno, P.V. Kamat, J. Am. Chem. Soc. 128 (2006) 2385.
[17] F. Denny, J. Scott, K. Chiang, W.Y. Teoh, R. Amal, J. Mol. Catal. A 263 (2006) 93.
[18] B. Sun, A.V. Vorontsov, P.G. Smirniotis, Langmuir 19 (2003) 3151.
[19] U. Siemon, D. Bahnemann, J.J. Testa, D. Rodríguez, M.I. Litter, N. Bruno, J. Photochem. Photobiol. A 148 (2002) 247.
[20] J. Lee, W. Choi, J. Phys. Chem. B 109 (2005) 7399.
[21] C.A. Emilio, M.I. Litter, M. Kunst, M. Bouchard, C. Colbeau-Justin, Langmuir 22 (2006) 3606.
[22] M.C. Hidalgo, M. Maicu, J.A. Navío, G. Colón, Catal. Today 129 (2007) 43.
[23] K.M. Schindler, M. Kunst, J. Phys. Chem. 94 (1990) 8222.
[24] G. Colón, M.C. Hidalgo, J.A. Navío, Appl. Catal. B 45 (2003) 39.
[25] S.S. Srinivasan, J. Wade, E.K. Stefanakos, Y. Goswami, J. Alloys Compd. 424 (2006) 322.
[26] S.P. Tandom, J.P. Gupta, Phys. Stat. Sol. 38 (1970) 363.
[27] M.A. Aramendía, J.C. Colmenares, A. Marinas, J.M. Marinas, J.M. Moreno, J.A. Navío, F.J. Urbano, Catal. Today 128 (2007) 235.
[28] I. Chorkendorff, J.W. Niemantsverdriet, Concepts of Modern Catalysis and Kinetics, Wiley–VCH Verlag, Weinheim, 2003.
[29] Z. Jin, Z. Chen, Q. Li, C. Xi, X. Zheng, J. Photochem. Photobiol. A 81 (1994) 177.
[30] G. Wang, Y. Lin, X. Xiao, X. Li, W. Wang, Surf. Int. Sci. 36 (2004) 1437.
[31] P. Panagiotopoulou, A. Christodoulakis, D.I. Kondarides, S. Boghosian, J. Catal. 240 (2006) 114.